Proceedings of Fifth International Conference on **Enhanced, Compact and Ultra-Compact Heat Exchangers: Science, Engineering and Technology**, Eds. R.K. Shah, M. Ishizuka, T.M. Rudy, and V.V. Wadekar, Engineering Conferences International, Hoboken, NJ, USA, September 2005.

CHE2005 – 50

Effects of Heat Exchanger Flow Channel Variations on Pressure Drop and Effectiveness due to Manufacturing and Fouling

Wei Shang and **Robert W. Besant**

University of Saskatchewan, Saskatoon, SK, Canada; wes153@mail.usask.ca

ABSTRACT

A significant concern with the design of ultra-compact heat exchangers is the impact on performance of flow channel variations due to manufacturing tolerances and fouling effects. As the flow channel diameters are decreased in any design, the impact of flow channel size variations is to decrease both the pressure drop and effectiveness. With flow channel fouling, however, the pressure drop increases with time while the effectiveness decreases with time. It is the purpose of this paper to investigate these performance changes in rotary heat exchangers with both finite manufacturing tolerances and fouling.

Measured data, used for manufacturing variations in regenerative wheels, are combined with analytical methods to predict the pressure drop and effectiveness decreases. Fouling, caused by frost growth, is measured indirectly to show how it increases the pressure drop and decreases the effectiveness.

It is concluded that the combined effects of manufacturing tolerances and fouling for the flow channels of heat exchangers both play an important role in altering the performance of heat exchangers. Experimental data and analytical methods are presented in this paper and used to interpret the resulting performance degradation of heat exchangers.

INTRODUCTION

With the development of manufacturing technologies to increase the surface area per unit volume, heat exchangers are manufactured with flow channel hydraulic diameters as small as 0.3 mm for HVAC applications (Shang and Besant, 2004a). These heat exchangers have a specific surface area of about 4,000 m^2/m^3 and about 40,000 flow channels per m^2 of face area. Kays and London (1984) classified these exchangers as compact heat exchangers. Four different flow channel geometries commonly used in HVAC applications are shown in Fig. 1. More recently, compact heat exchangers have been classified into micro-heat exchangers, meso-heat exchangers, compact heat exchangers, and conventional heat exchangers according to flow channel hydraulic diameters (Mehendale et al., 2000), i.e., $D_h = 1 - 100\ \mu m$, $D_h = 0.0001 - 1$ mm, $D_h = 1 - 6$ mm, and $D_h > 6$ mm respectively.

Shang and Besant (2004a) showed that the flow channel hydraulic diameter in regenerative exchangers reveal a Gaussian variation after construction due to manufacturing tolerances. Compared to regenerative exchangers with no variations in the flow channels, the performance deterioration of regenerative exchangers can be predicted when these manufacturing flow channel variations are known (Shang and Besant, 2005).

In application, heat exchangers are often exposed to fluids that chemically alter or deposit solid materials on the exchange surfaces. These deposits add a fouling resistance to the heat exchanger surfaces and blocks or obstructs the flow channel area (Philips, 1990). For example, dust particles, smaller than a filter size, can gradually deposit to reduce or clog flow channels and ice crystal deposition in the form of frost can quickly reduce the performance of any exchanger. Although there has been no mention of fouling for micro-/meso-heat exchangers (Mehendale, 2000), it is well

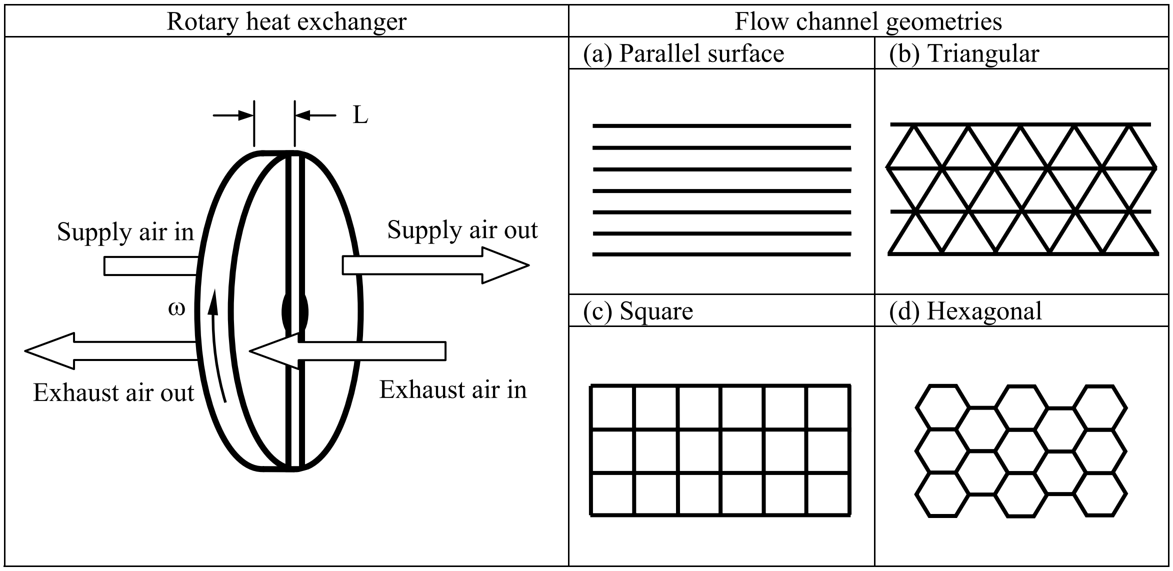

Fig. 1 A typical rotary heat exchanger and four different flow channel geometries

understood that the smaller the flow channel sizes the larger the impact due to fouling.

It is the purpose of this paper to show that manufacturing variations and fouling effects on flow channel size variations, which often occur in applications, can be separated for measurement and analysis — so their combined effect on performance can be analyzed. First, a rotary heat exchanger with measured variations in the flow channels and a mean hydraulic diameter of 1.00 mm will be considered and then the fouling effects of frost growth are measured for certain selected inlet properties for the same exchanger. Frost growth inside the flow channels was investigated because of its many practical applications and very rapid growth rate.

Performance of Heat Exchangers

To characterize the performance of a rotary heat exchanger, several performance factors are needed. ASHRAE Std 84-91R, requires the measured determination of effectiveness, ε, pressure drop, Δp, EATR (Exhaust Air Transfer Ratio), OACF (Outside Air Correction Factor), and RER (Recovery Efficiency Ratio). Among these factors, the effectiveness, ε, and pressure drop, Δp, are of greatest concern to manufacturers and application engineers. Below we show how manufacturing tolerances and fouling effects alter the effectiveness, ε, and pressure drop, Δp for a rotary heat exchanger.

The calculation of the effectiveness of a heat exchanger is presented in ASHRAE Std 84-91R. The

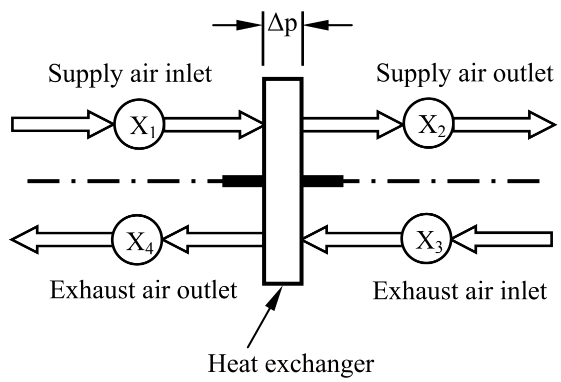

Fig. 2 Schematic for counter-flow heat exchangers and the measuring stations X_1 to X_4

measurement is performed at the four stations as shown in Fig. 2. When the variations in specific heat are negligible, the sensible energy effectiveness for a heat exchanger is defined as

$$\varepsilon_s = \frac{\dot{m}_s (T_1 - T_2)}{\dot{m}_{min} (T_1 - T_3)} \tag{1}$$

where

T = dry-bulb temperature (K),

$\dot{m}_s$ = mass flow rate of dry air in the supply stream (kg/s),

$\dot{m}_e$ = mass flow rate of dry air in the exhaust stream (kg/s),

$\dot{m}_{min}$ = minimum value of either $\dot{m}_s$ or $\dot{m}_e$ (kg/s).

For balanced flows in the supply and exhaust streams, $\dot{m}_s = \dot{m}_e = \dot{m}_{min}$, Eq. (1) can be simplified as

$$\varepsilon_s = \frac{(T_1 - T_2)}{(T_1 - T_3)} \tag{2}$$

In this study, the actual performance factors, Δp and ε, are compared with the ideal design values for an identical rotary exchanger with no flow channel variations, operating under the same inlet conditions of temperature, humidity, and mass flow rate of dry air. This ideal exchanger, with no variations between flow channels and no fouling, has the ideal pressure drop, Δp^*, and sensible effectiveness, ε^*. Then the ratios $\Delta p / \Delta p^*$ and $\varepsilon / \varepsilon^*$ are new measures of the exchanger performance. If there is no fouling, but there is a variation of flow channel sizes due to manufacturing tolerances these new performance factors will not change with time unless the inlet flow properties change. Then

$$\frac{\Delta p}{\Delta p^*} = \frac{\Delta p_0}{\Delta p^*} \tag{3}$$

and

$$\frac{\varepsilon}{\varepsilon^*} = \frac{\varepsilon_0}{\varepsilon^*} \tag{4}$$

where Δp_0 is the pressure drop and ε_0 is the effectiveness when there is no fouling. When fouling effects are combined with manufacturing tolerances, both Δp and ε will vary with time and we can write these new performance factors as

$$\frac{\Delta p(t)}{\Delta p^*} = \frac{\Delta p_0}{\Delta p^*} \cdot \frac{\Delta p(t)}{\Delta p_0} \tag{5}$$

and

$$\frac{\varepsilon(t)}{\varepsilon^*} = \frac{\varepsilon_0}{\varepsilon^*} \cdot \frac{\varepsilon(t)}{\varepsilon_0} \tag{6}$$

where $\Delta p(t)/\Delta p_0$ will be the change in the pressure drop ratio with time due to fouling compared to the same exchanger with none, and $\varepsilon(t)/\varepsilon_0$ will be the corresponding effectiveness ratio due to fouling compared to the same exchanger with none.

EFFECTS OF MANUFACTURING TOLERANCES ON HEAT EXCHANGER PERFORMANCE

The flow channel hydraulic diameters in these heat exchangers have been found to exhibit a Gaussian distribution (Shang and Besant, 2004a), with a mean hydraulic diameter, D^*, and standard deviation, σ_0. The Reynolds number for the flows within the flow channels are in the range of $200 < Re < 1000$.

Assuming only fully developed laminar flow (Shang and Besant, 2005), random variations in the flow channel hydraulic diameters which are each of similar parallel surface or cylindrical shape, and equal mass flow rates through the actual rotary heat exchanger and the comparative ideal exchanger with only the mean hydraulic diameter of flow channels, D^*, an analytical equation can be derived to relate the pressure drop across the flow channels with variations, Δp_0, to the pressure drop across the flow channels without variations, Δp^*. This relationship is

$$\frac{\Delta p_0}{\Delta p^*} = F_1\left(\frac{\sigma_0}{D^*}\right) \tag{7}$$

Equation (7) does not consider the fouling effects on pressure drop but it does include flow channel manufacturing tolerances. For example, for an exchanger matrix manufactured with parallel surface flow channels:

$$\frac{\Delta p_0}{\Delta p^*} = \left[1 + \left(\frac{\sigma_0}{D^*}\right)^2\right]^{-1} \tag{8}$$

and for symmetrical cylinder type flow channels (i.e., equilateral triangle, square, hexagonal, and circular flow channels):

$$\frac{\Delta p_0}{\Delta p^*} = \left[1 + 6\left(\frac{\sigma_0}{D^*}\right)^2 + 3\left(\frac{\sigma_0}{D^*}\right)^4\right]^{-1} \tag{9}$$

Figure 3 shows the relationship between the pressure drop ratio and σ_0 / D^* for different flow channel geometries. The dark line shows the pressure drop with increasing σ_0 / D^* for a heat exchanger with a parallel surface matrix. For heat exchangers with matrices with symmetrical cylinder type flow channels, such as equilateral triangle, square geometry, hexagonal, or circular cylinder geometry, the pressure drop ratio is presented by the dashed curve.

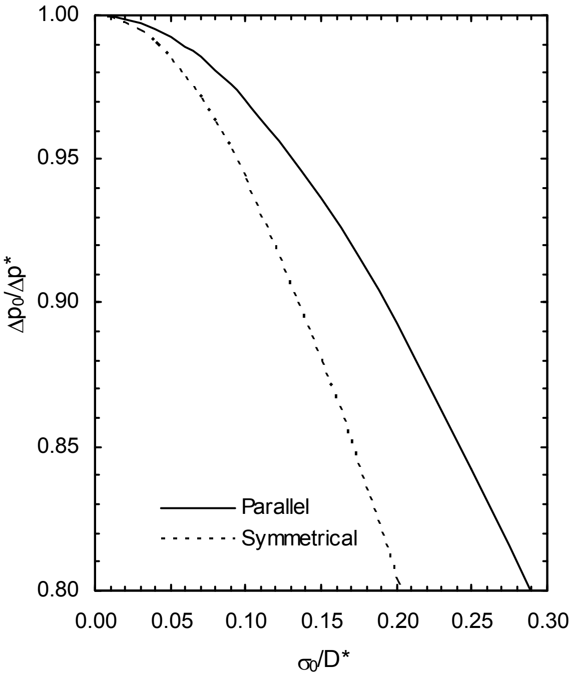

Fig. 3 Pressure drop ratios for heat exchangers with a matrix of parallel surface flow channels and a matrix containing symmetrical cylinder flow channels (i.e., equilateral triangle, square, hexagonal, or circular flow channels) with random variations in flow channel sizes to one without versus the standard deviation in flow channel hydraulic diameters with respect to the mean value

Similarly, at any operating condition the effectiveness ratio, $\varepsilon_0/\varepsilon^*$, of the heat exchanger with flow channel size variations and without variations can be expressed as

$$\frac{\varepsilon_0}{\varepsilon^*} = F_2\left(\frac{\sigma_0}{D^*}, \partial\varepsilon_m\right) \tag{10}$$

where $\partial\varepsilon_m$ is the effectiveness sensitivity coefficient defined by

$$\partial\varepsilon_m = \frac{\dot{m}}{\varepsilon^*}\frac{\partial\varepsilon}{\partial\dot{m}}\bigg|_{\dot{m}} \tag{11}$$

$\partial\varepsilon_m$ is a constant for each specified operating condition and it can be assumed to be constant over a wide range of operating conditions (Shang and Besant, 2005).

Figure 4 shows the effectiveness ratios are determined by knowing the flow channel size variations and operating conditions for a rotary heat exchanger with a matrix of parallel surfaces (solid curves) and a rotary heat exchanger with symmetrical cylinder type flow channels (dashed curves). In most HVAC applications, $\partial\varepsilon_m$ has a value close to -0.3 and a range $-0.5 < \partial\varepsilon_m < -0.1$ would cover almost all typical operating conditions for rotary heat and energy exchangers.

A heat exchange process in a heat exchanger will cause a net increase in the entropy of the two flowing air streams (Bejan, 1997). For ideal gases, flowing in counterflow with equal mass flow rates through a rotary heat exchanger rotating at a speed high enough so that the effectiveness depends only on the dimensionless number of transfer units (Ntu)

$$\varepsilon = \frac{Ntu}{1+Ntu} = \frac{(T_1 - T_2)}{(T_1 - T_3)} = \frac{(T_4 - T_3)}{(T_1 - T_3)} \tag{12}$$

The dimensionless entropy generation number for the two air streams can be written as (Bejan, 1997)

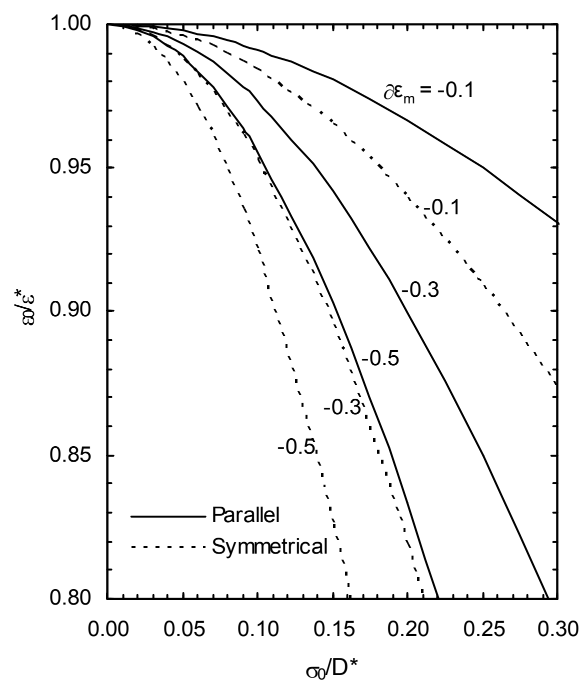

Fig. 4 Effectiveness ratio for heat exchangers with a matrix of parallel surface flow channels and a matrix containing symmetrical cylinder flow channels (i.e., equilateral triangle, square, and hexagonal, or circular flow channels) with random variations in flow channel sizes to one without versus the standard deviation in flow channel hydraulic diameters with respect to the mean value

Table 1 Certification operating conditions for air-to-air exchanger tests, ARI Std 1060-2001

Item	Test conditions	
	Summer cooling	Winter heating
(1) Entering supply air		
(a) Dry bulb temperature	35 ± 1°C (95 ± 1.8°F)	1.7 ± 1°C (35 ± 1.8°F)
(b) Relative humidity	47.4% ± 2%	82.5% ± 2%
(2) Entering exhaust air		
(a) Dry bulb temperature	23.9 ± 1°C (75 ± 1.8°F)	21.1 ± 1°C (70 ± 1.8°F)
(b) Relative humidity	51.2% ± 2%	49.2% ± 2%

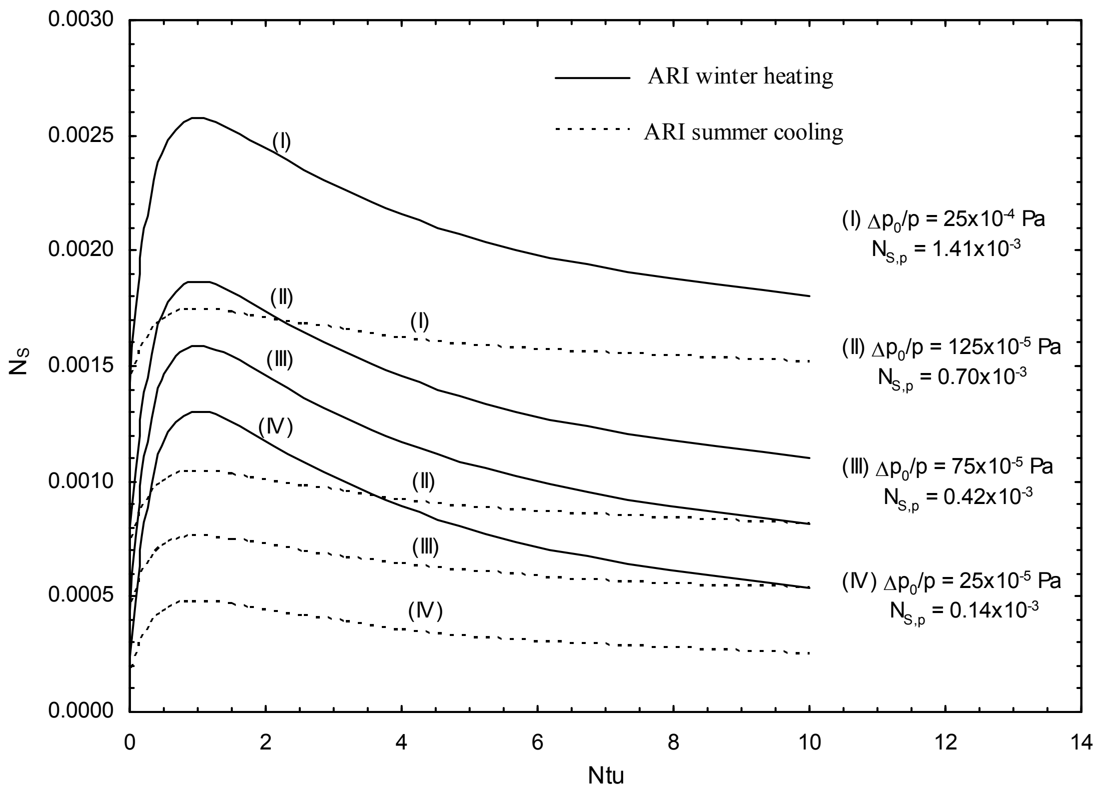

Fig. 5 Entropy generation number versus number of transfer units for the conditions of ARI summer cooling test and winter heating tests as shown in Table 1

$$N_S = \frac{\dot{S}_{gen}}{\dot{m}c_p} = \ln\frac{T_2}{T_1} + \ln\frac{T_4}{T_3} - \frac{R}{c_p}\left(\ln\frac{p_2}{p_1} + \ln\frac{p_4}{p_3}\right) \tag{13}$$

where c_p is assumed to be constant and any water vapour transfer between the two air streams is negligible.

Substituting Eq. (12) into Eq. (13) and expanding the ln terms as infinite series

$$N_S = \theta\varepsilon - \frac{1}{2}(\theta\varepsilon)^2(\theta_M^2 + \theta_m^2) + \frac{1}{3}(\theta\varepsilon)^3(\theta_M^3 - \theta_m^3) - \frac{1}{4}(\theta\varepsilon)^4(\theta_M^4 + \theta_m^4) + \cdots + \frac{R}{c_p}\left(\frac{\Delta p_{1-2}}{p_1} + \frac{\Delta p_{3-4}}{p_3}\right) \tag{14}$$

where it is assumed that $\Delta p / p << 1$, as it is for practical applications. Then

$$N_S = \theta\varepsilon - \sum_{n=2}^{\infty}(-1)^n \frac{(\theta\varepsilon)^n}{n}[(-1)^n \theta_m^n + \theta_M^n] + \frac{R}{c_p}\frac{2\Delta p}{p}$$
$$= N_{S,T} + N_{S,p} \tag{15}$$

which are the heat transfer and pressure-drop terms respectively and where the temperature ratios, θ_M, θ_m, and θ, are defined as

$$\theta_M = \text{max of}\left\{\frac{T_1}{\Delta T_M}, \frac{T_3}{\Delta T_M}\right\} \tag{16}$$

$$\theta_m = \text{min of}\left\{\frac{T_1}{\Delta T_M}, \frac{T_3}{\Delta T_M}\right\} \tag{17}$$

$$\theta = \frac{1}{\theta_M}\cdot\frac{1}{\theta_m} \tag{18}$$

where

$$\Delta T_M = |T_1 - T_3| \tag{19}$$

We assume that the pressure drops for either flow channels are the same and the absolute pressures entering either flow channels are equal, i.e.:

$$\Delta p = \Delta p_{1-2} = \Delta p_{3-4} \tag{20}$$

$$p = p_1 = p_3 = p_{atm} \tag{21}$$

The typical operating conditions for heat exchanger performance tests are presented in Table 1 which are from ARI Std 1060. Under these ARI certification test conditions, the entropy generation number versus number of transfer units is presented in Fig. 5. This figure shows that N_S has a peak value at $Ntu = 1.0$ and declines to a smaller value as $Ntu \to 0$ or as Ntu increases to a large value.

Further analysis of the entropy generation number, N_S, with variations in flow channel hydraulic diameter shows that significant changes to N_S occur as σ_0 / D^* increases and both $N_{S,T}$ and $N_{S,p}$ play important roles (Shang and Besant, 2004b).

FOULING EFFECTS ON PRESSURE DROP RATIO

The pressure drop ratio due to manufacturing tolerances and fouling effects inside a heat exchanger can be expressed as

$$\frac{\Delta p(t)}{\Delta p^*} = F_1\left(\frac{\sigma_0}{D^*}\right)\cdot F_{1f}(t) \tag{22}$$

where

$$F_1\left(\frac{\sigma_0}{D^*}\right) = \frac{\Delta p_0}{\Delta p^*} \tag{23}$$

is the pressure drop ratio due to flow channel hydraulic diameter variations caused by manufacturing tolerances.

$$F_{1f}(t) = \frac{\Delta p(t)}{\Delta p_0} \tag{24}$$

is the ratio of the pressure drop across the flow channels at any time compared to the pressure drop at $t = 0$. $F_{1f}(t)$ is the fouling function for pressure drop of the heat exchanger. This fouling function is dependent on the operating environment and it must be determined by pressure difference measurements.

For fouling due to frost accumulation in flow channels, Eq. (24) can be written in the functional form of

$$F_{1f}(t) = F_{1f2}(t)\cdot F_{1f3}\left(\frac{\sigma}{\overline{D}}\right) \tag{25}$$

where $\overline{D}$ is the mean air flow hydraulic diameter of the flow channels with frost accumulation and

$$F_{1f2}(t) = \frac{\Delta p_{\overline{D}(t)}}{\Delta p_0} \tag{26}$$

is the temporal relative increase in pressure drop (assuming the fouling is identical in each flow channel) and

$$F_{1f3}\left(\frac{\sigma}{\overline{D}}\right) = \frac{\Delta p(t)}{\Delta p_{\overline{D}(t)}} \tag{27}$$

is the pressure drop ratio decrease at any time due to variations in the flow channel hydraulic diameters caused by fouling.

FOULING EFFECTS ON EFFECTIVENESS RATIO

The effectiveness ratio due to manufacturing tolerances and fouling effects in a heat exchanger can be expressed as

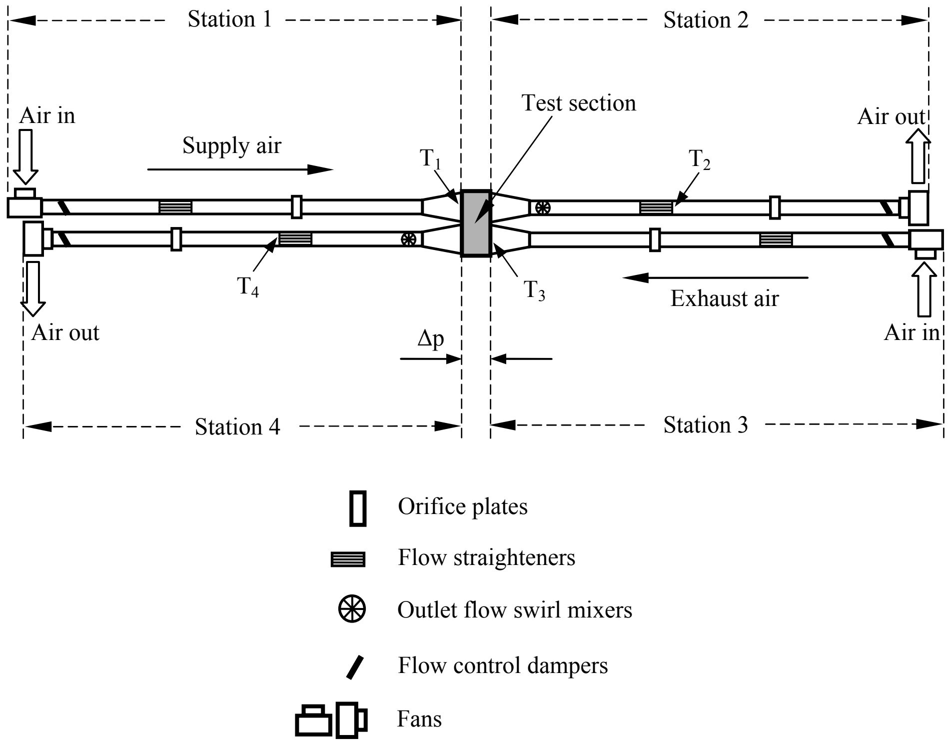

Fig. 6 A schematic diagram of the laboratory experimental test facility and instrumentation for a typical rotary heat exchanger for fouling due to frost growth effects

$$\frac{\varepsilon(t)}{\varepsilon^*} = F_2\left(\frac{\sigma_0}{D^*}, \partial\varepsilon_m\right) \cdot F_{2f}(t) \tag{28}$$

where

$$F_2\left(\frac{\sigma_0}{D^*}, \partial\varepsilon_m\right) = \frac{\varepsilon_0}{\varepsilon^*} \tag{29}$$

is the effectiveness ratio due to manufactured flow channel size variations and

$$F_{2f}(t) = \frac{\varepsilon(t)}{\varepsilon_0} \tag{30}$$

is the effectiveness ratio due to fouling. $\varepsilon(t)$ is the effectiveness of the heat exchanger at any time after fouling has started and this is written as a quasi-steady-state form of Eq. (2)

$$\varepsilon(t) = \frac{T_1 - T_2(t)}{T_1 - T_3} \tag{31}$$

where

$$\varepsilon_0 = \varepsilon(t = 0) \tag{32}$$

Similar to the changes in measured pressure drop due to fouling effects, the effects of fouling on heat rate must be measured and this is best presented as an effectiveness $\varepsilon(t)$ of an effectiveness ratio $\varepsilon(t)/\varepsilon_0$.

TEST FACILITY, INSTRUMENTATION, AND OPERATING CONDITION

Tests for fouling of heat exchangers can be extremely time consuming in a laboratory, because it may take weeks, months, or years of testing to collect enough data to calculate performance changes. To avoid the problem mentioned above, a laboratory test facility for fouling was set up for frost fouling of a rotary heat exchanger as shown in Fig. 6. This set up conforms to the ASHRAE Std 84-91R for steady-state testing of an air-to-air exchanger.

The conditions for the fouling test are presented in Table 2. During these tests, the frost grows within the heat exchanger when the humid and warm exhaust air cools below the dew point while the dry and cold supply air is heated. The air temperatures were measured at stations 1 to 4 as shown in Fig. 6.

Table 2 Test conditions

	Temperature (^{o}C)	Humidity ratio (kg/kg)	Dry air mass flux (kg/m^2 s)	Wheel speed (rpm)
Supply air	-40	0.00004	2.41	20
Exhaust air	+20	0.0058	2.41	20

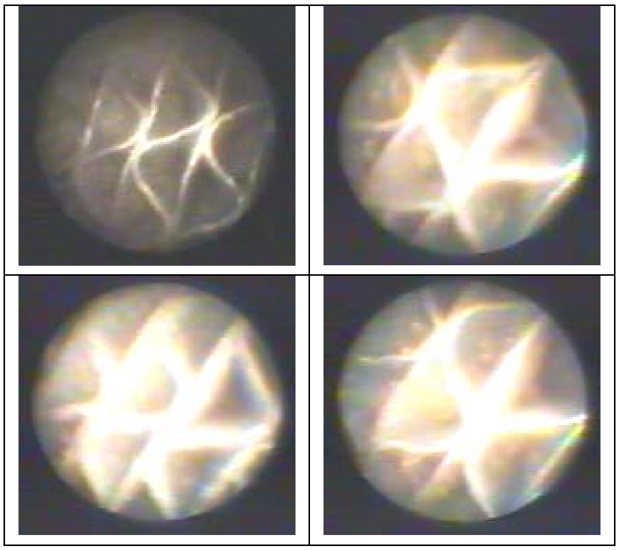

Fig. 7 Photos of flow channels of the heat exchanger: (a) before fouling; (b), (c), and (d) after 30 minutes fouling started due to frost growth in the flow channels

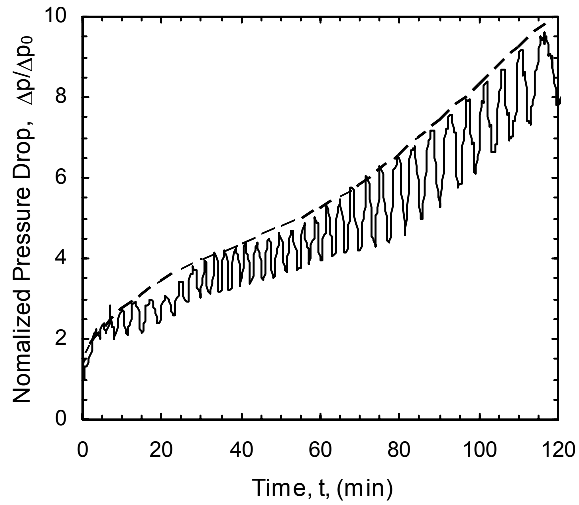

Fig. 8 Pressure drop ratio across the rotary heat exchanger versus time

Under the very cold supply air operating conditions in Table 2, the fouling occurred rapidly and the air flow rate had to be carefully controlled to maintain a constant mass flow of dry air for both the supply and exhaust. Figure 7 shows the photos before fouling and after fouling.

MEASURED DATA AND RESULTS

The pressure drop across the heat exchanger was measured using static pressure probes and a manometer. Before the frost growth, the initial pressure drop was $\Delta p_0 = 37 \pm 5$ Pa. The normalized pressure drop or the pressure fouling function is presented in Fig. 8. As shown in Fig. 8 the dark line is from the data of pressure drop during the 120 minutes of frost growth. The dashed line represents the upper limit of the pressure drop cyclic variations. These pressure drop variations were caused by frost fracturing which had a cycle period of 3 to 4 minutes. These measured results imply that frost fracturing in the flow channels reduces the pressure drop when a significant fraction of the flow channels experiences frost fracture. This occurs over half of the cyclic pressure drop variations or 1.5 to 2 minutes of pressure drop decrease. Each of these pressure drop declines was followed by a pressure rise caused by rapid frost growth for 1.5 to 2 minutes.

If we interpret these frost cycle variations as flow channel hydraulic diameter variations using the same theory as for manufacturing tolerances, we can estimate the magnitude of these variations using the standard deviation to mean value of diameter as a parameter. This is done in Fig. 9 which shows that the pressure drop ratios for $\sigma_0 / D^* = 0.05$, 0.15, and 0.25 under the same fouling operating condition. That is the peak pressure drop coincides with $\sigma_0 / D^* = 0.05$ while the minimum pressure drop for each cycle coincides well with $\sigma_0 / D^* = 0.25$.

These results do not mean that flow channel hydraulic diameter variations would not occur if there were no frost fracturing. The entropy generation number always decreases for high pressure drop when there are flow channel size variations. Frost fracturing simply increases these variations to very large values.

Figure 10 shows the temperatures at the four stations, 1 to 4. The temperatures at the inlets were kept

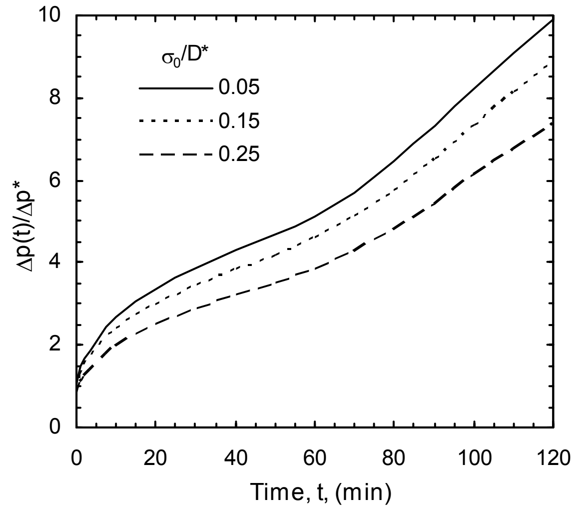

Fig. 9 Pressure drop ratio for the heat exchanger versus time

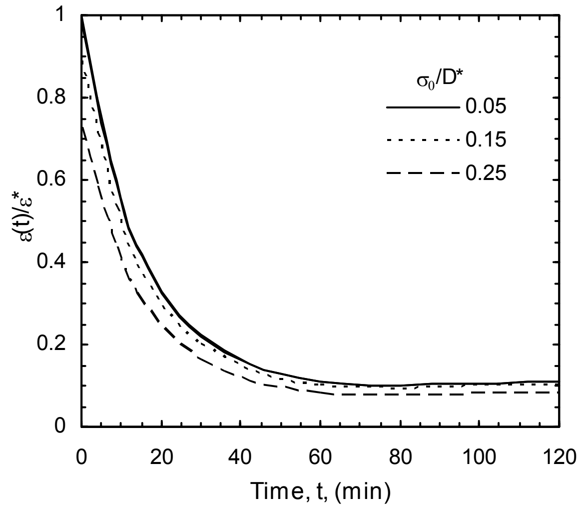

Fig. 11 Effectiveness ratio for the heat exchanger versus time

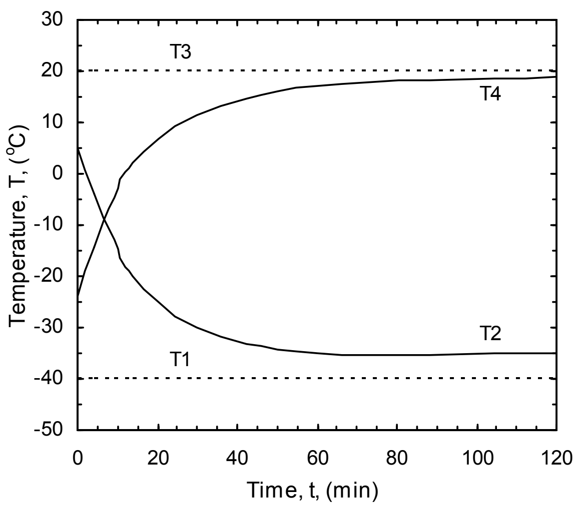

Fig. 10 Measured data for temperatures at stations 1 to 4 versus time

at constant conditions. The temperature at the supply air outlet decreased and the temperature at the exhaust air outlet increased due to fouling impacts, i.e., frost growth within the heat exchanger.

Figure 11 shows the effectiveness ratio for $\sigma_0 / D^* = 0.05$, 0.15, and 0.25 under the same operating condition. It is concluded from this figure, that although the pressure drop cycles are large, the corresponding effectiveness variations will be small compared to the uncertainty in the measurements.

It is known that the entropy generation number, N_S, is important for flows that have multiple and branched flow paths (Bejan, 1997). With frost growth, the mass of frost can be distributed at any time so that N_S tends toward a smaller value. This will occur when the flow channel diameters are not uniformly coated in frost.

SUMMARY AND CONCLUSIONS

Both manufacturing tolerances and fouling effects can impact the performance of heat exchangers. The effects of manufacturing and fouling on heat exchanger performance can be considered and analyzed separately.

Manufacturing and fouling play different roles on pressure drop across heat exchangers. The impacts on the effectiveness of heat exchangers due to manufacturing and fouling are the same and always decrease the value of effectiveness. For example, if the manufacturing tolerance results in $\sigma_0 / D^* = 0.10$, then the effectiveness ratio, $\varepsilon_0 / \varepsilon^* = 0.95$ for $\partial\varepsilon_m = -0.3$. Manufacturing tolerance always decreases the pressure drop; but fouling increases the pressure drop even though significant variations in the flow channel hydraulic diameters may exist. When frost fouling is allowed to persist over a time period to cause a large fraction of flow channel blocking to occur, frost fracturing will occur which is manifested as large amplitude pressure drop fluctuations. When these cyclic fluctuations are analyzed as flow channel hydraulic diameter variations they correspond to a standard deviation to mean diameter ratio of 0.25.

NOMENCLATURE

c_p = specific heat, J/kg K
D = hydraulic diameter of flow channels, m
D^* = mean hydraulic diameter of flow channels, m
$\overline{D}(t)$ = mean air flow hydraulic diameter at time, t, m
F_l = pressure drop ratio function due to manufacturing tolerances, dimensionless
F_{lf} = pressure drop ratio function due to fouling effects, dimensionless
F_{lf2} = pressure drop ratio function due to fouling effects for frost accumulation, defined by Eq. (26), dimensionless
F_{lf3} = pressure drop ratio function due to fouling effects for frost accumulation, defined by Eq. (27), dimensionless
F_2 = effectiveness ratio function due to manufacturing tolerances, dimensionless
F_{2f} = effectiveness ratio function due to fouling effects, dimensionless
L = length of flow channel or thickness of a rotary heat exchanger, m
$\dot{m}$ = mass flow rate of dry air, kg/s
N = number of flow channels in a rotary heat exchanger, dimensionless
N_S = entropy generation number, dimensionless
Ntu = number of transfer units, dimensionless
p = pressure, Pa
Δp = pressure drop, Pa
Δp_0 = pressure drop across a heat exchanger with nonuniform flow channels, Pa
Δp^* = pressure drop across a heat exchanger with uniform flow channels, Pa
R = universal gas constant, dimensionless
Re = Reynolds number, dimensionless
$\dot{S}$ = entropy generation rate, W/K
t = time, min
T = temperature, K
V = mean flow velocity, m/s
W = humidity ratio, kg/kg

Greek

ε = heat exchanger effectiveness, dimensionless
ε_0 = effectiveness for a heat exchanger with non-uniform flow channels, dimensionless
ε^* = effectiveness for a heat exchanger with uniform flow channels, dimensionless
$\partial\varepsilon_m$ = effectiveness sensitivity coefficient, dimensionless
θ = non-dimensional temperature, dimensionless
ω = wheel speed, rad/s
σ = standard deviation of air flow hydraulic diameters, m
σ_0 = standard deviation of flow channel hydraulic diameters, m

Subscripts

atm = atmospheric
e = exhaust air
f = fouling
gen = entropy generation
h = hydraulic diameter
M = maximum value
m = mass flow or minimum value
min = minimum value
p = pressure
S = entropy
s = supply air or sensible energy
T = relating to temperature variation
0 = mean value for all flow channels
1 = station 1
2 = station 2
3 = station 3
4 = station 4

ACKNOWLEDGEMENTS

Funding for this research work was provided by enmar CES, and NSERC, Canada. The regenerative exchangers used for testing were provided by Venmar CES, Saskatoon, SK, Canada.

REFERENCES

ARI, 2001, *ARI Standard 1060: Rating Air-to-Air Energy Recovery Ventilation Equipment*, Air-Conditioning & Refrigeration Institute, Arlington, Virginia.

ASHRAE, 1991, *ANSI/ASHRAE Standard 84-1991R, Method of Testing Air-to-Air Heat Exchangers*, American Society of Heating, Refrigerating and Air-Conditioning Engineers, Inc., Atlanta, GA.

Bejan, A., 1997, *Advanced Engineering Thermodynamics*, Wiley, New York.

Mehendale, S. S., A. M. Jacobi, A. M., and R. K. Shah, R. K., 2000, Fluid Flow and Heat Transfer at Micro- and Meso-scales with Application to Heat Exchanger Design, *Applied Mechanics Reviews*, **53**, pp. 175–193.

Philips, R. J., 1990, Microchannel Heat Sinks, in *Advances in Thermal Modeling of Electronic Components and Systems*, A. Bar-Cohen and A. D. Kraus, eds., ASME, New York.

Shang, W. and Besant, R. W., 2004a, Measurement of Pore Size Variation and Its Effect on Energy Wheel Performance, *ASHRAE Trans*., **110**(1), pp. 410–421.

Shang, W. and Besant, R. W., 2004b, Effects of Manufacturing Tolerances on Regenerative Exchanger Number of Transfer Units and Entropy Generation, Submitted for Publication in *ASME J. Eng. Gas Turbines Power*.

Shang, W. and Besant, R. W., 2005, Effects of Pore Size Variations on Regenerative Wheel Performance, *ASME J. Eng. Gas Turbines Power*, **127**(1), pp. 1–15.